Models, parameters, and approaches that used to generate wide range of absorption and backscattering spectra

Ocean Color Algorithm Working Group
IOCCG
June 2003

1. Objective

Generate a comprehensive data set for algorithm test/comparison. This data set contains both inherent optical properties (IOPs) and apparent optical properties (AOPs). The focus will be just on the derivation of IOPs from AOPs, such as absorption coefficient of the total and individual components, particle backscattering, etc.

2. Approach

IOPs are generated with various available/reasonable optical/bio-optical parameters/models, while AOPs are generated using HydroLight with the available IOPs.

3. Optical and bio-optical models/parameters for IOP

As earlier studies [*Bukata et al.*, 1995; *Carder et al.*, 1991; *Doerffer et al.*, 2002; *Fischer and Fell*, 1999; *Prieur and Sathyendranath*, 1981; *Roesler et al.*, 1989], a four-component model is used to generate IOPs of the bulk water. Specifically, absorption (a) and backscattering (bb) coefficients are described as

$$\begin{aligned} a(\lambda) &= a_{\mathrm{w}}(\lambda) + a_{ph}(\lambda) + a_{dm}(\lambda) + a_{\mathrm{g}}(\lambda) \\ bb(\lambda) &= bb_{\mathrm{w}}(\lambda) + bb_{\mathrm{ph}}(\lambda) + bb_{dm}(\lambda) \end{aligned} . \qquad (1)$$

$a_{\mathrm{w}}(\lambda)$ from Pope and Fry [*Pope and Fry*, 1997] and $bb_{\mathrm{w}}(\lambda)$ from Morel [*Morel*, 1974] at defined temperature and salinity are used.

Phytoplankton concentration, [C], will be used as the free parameter to define different waters. [C] is set in a range of 0.03 – 30.0 μg/l with 20 steps (see Table 1), and for each step there are 25 [C] values to create different absorption and backscattering values. In total, there are 500 IOP data points.

3.1 absorption term

3.1.1 Phytoplankton pigment absorption, $a_{ph}(\lambda)$

$a_{ph}(\lambda)$ is expressed as

$$a_{ph}(\lambda) = a_{ph}(440)\, a^{+}_{ph}(\lambda), \tag{2}$$

with $a^{+}_{ph}(\lambda)$ the $a_{ph}(440)$-normalized spectral shape. For each $[C]$ value, $a_{ph}(440)$ is created [*Bricaud et al.*, 1995; *Fischer and Fell*, 1999] with

$$a_{ph}(440) = 0.05\ [C]^{0.626}. \tag{3}$$

Note that the parameters 0.05 and 0.626 can vary a lot from place to place. These values here are merely to get the reasonable values and range of $a_{ph}(440)$. Since the focus of this data set is to test the inversion of IOPs, how $a_{ph}(440)$ exactly vary with $[C]$ is not that important, as long as $a_{ph}(440)$ values are reasonable.

$a^{+}_{ph}(\lambda)$ spectrum comes from the extensive measurements of Bricaud et al. [*Bricaud et al.*, 1995; *Bricaud et al.*, 1998] and Carder et al. [*Carder et al.*, 1999]. This $a^{+}_{ph}(\lambda)$ data bank (600 spectra) is divided into nine groups, separated by the measured $a_{ph}(440)$ values. For a given $a_{ph}(440)$, $a^{+}_{ph}(\lambda)$ is selected randomly [Doerffer, personal communication] from the corresponding group.

3.1.2 Detritus/mineral (non-algae colored particulate matter) absorption, $a_{dm}(\lambda)$

$a_{dm}(\lambda)$ spectrum is modeled as Roesler et al. [*Roesler et al.*, 1989] and Bricaud et al. [*Bricaud et al.*, 1995], i.e.,

$$a_{dm}(\lambda) = a_{dm}(440)\exp(-S_{dm}(\lambda - 440)), \tag{4}$$

with S_{dm} randomly valued between 0.007 and 0.015 nm^{-1} [*Babin et al.*, 2003; *Roesler et al.*, 1989] for each $[C]$.

$a_{dm}(440)$, the detritus absorption at the reference wavelength, is randomly determined for each $[C]$. This randomness, however, is constrained based on observations. Define p_1 as the ratio of $a_{dm}(440)/a_{ph}(440)$, then

$$a_{dm}(440) = p_1\, a_{ph}(440), \tag{5}$$

with p_1 generated from

$$p_1 = 0.1 + \frac{0.5\,\Re_1\,a_{ph}(440)}{0.05 + a_{ph}(440)}. \quad (6)$$

Here $\Re_1$ is a random value between 0 and 1 (makes p_1 in a range of 0.1 – 0.6). This way there will be no extremely large $a_{dm}(440)$ values when $a_{ph}(440)$ values are small. Also, as $\Re_1$ is a random value, the relationship between $a_{dm}(440)$ and $a_{ph}(440)$ is not fixed, as observed in the field. Figure 1 presents the distribution of p_1 values, which shows wider p_1 range for larger $a_{ph}(440)$ values (higher concentration).

3.1.3 Gelbstoff (colored dissolved organic matter) absorption, $a_g(\lambda)$

$a_g(\lambda)$ spectrum is modeled as Bricaud et al. [*Bricaud et al.*, 1981],

$$a_g(\lambda) = a_g(440)\exp(-S_g(\lambda - 440)), \quad (7)$$

with S_g randomly valued between 0.01 – 0.02 nm^{-1} [*Babin et al.*, 2003; *Kirk*, 1994] for each [*C*] value.

$a_g(440)$, the gelbstoff absorption at the reference wavelength, is also randomly determined for each [*C*] value. This randomness is also constrained based on observations. Define p_2 as the ratio of $a_g(440)/a_{ph}(440)$, then

$$a_g(440) = p_2\,a_{ph}(440), \quad (8)$$

with p_2 generated from

$$p_2 = 0.3 + \frac{5.7\,\Re_2\,a_{ph}(440)}{0.02 + a_{ph}(440)}. \quad (9)$$

Again, $\Re_2$ is a random value between 0 and 1 (makes p_2 in a range of 0.3 – 6.0). This way there will be no extremely large $a_g(440)$ values when $a_{ph}(440)$ values are small. Also, as $\Re_2$ is a random value, the relationship between $a_g(440)$ and $a_{ph}(440)$ is not fixed, as observed in the field. The upper limit of 6.0 may not cover extreme cases, but should be large enough to cover most sea waters. Figure 2 presents the distribution of p_2 values. Note the wider range of p_2 values for higher $a_{ph}(440)$ values.

Since p_2 is in a random range of 0.3 – 6.0, the dominant absorber in the short wavelengths could be either a_{ph} or a_g, especially for water with higher concentrations. For lower concentrations, values of p_1 and p_2 are in the lower-narrower range, consistent with open-ocean waters.

Figure 3 shows the values of $a(440)$ of the data set. Since p_1 and p_2 are wide range random values, multiple $a(440)$ values are obtained for the same [C] values, as observed in the field.

3.2 backscattering term

3.2.1 backscattering of phytoplankton, $bb_{ph}(\lambda)$

Following Bukata et al. [*Bukata et al.*, 1995], Stramski et al. [*Stramski et al.*, 2001] and Roesler and Boss [*Roesler and Boss*, 2003], $bb_{ph}(\lambda)$ is modeled as

$$\begin{aligned} bb_{ph}(\lambda) &= \tilde{b}_{ph}\, b_{ph}(\lambda) \\ b_{ph}(\lambda) &= c_{ph}(\lambda) - a_{ph}(\lambda) \quad . \\ c_{ph}(\lambda) &= c_{ph}(550)\left(\frac{550}{\lambda}\right)^{n1} \end{aligned} \tag{10}$$

Values of $\tilde{b}_{ph}$ depends on the phase function of phytoplankton, here a 1% bb/b Fournier-Forand function is selected, which is consistent with the recent measurements of Oishi et al. [*Oishi et al.*, 2002]. $c_{ph}(550)$ and n_1 for a given [C] need to be determined. $c_{ph}(550)$ is modeled as [*Voss*, 1992]

$$c_{ph}(550) = p_3 [C]^{0.57}, \tag{11}$$

with p_3 randomly valued between 0.06 and 0.6 for a given [C] value.

n_1 is generated with

$$n_1 = -0.4 + \frac{1.6 + 1.2\,\Re_3}{1 + [C]^{0.5}}. \tag{12}$$

Here $\Re_3$ is a random value between 0 and 1. n_1 is in a range of -0.1 to 2.0 [*Sathyendranath et al.*, 1989], but varies randomly for each [C]. Basically Eq.12 allows n_1 decreases with increase of [C] but in a random fashion. And for a given [C] value, the generated n_1 value varies in a factor of 2. Figure 4 presents the distribution of n_1, lower for higher concentrations (presumably coastal waters), and higher for lower concentrations (presumably open-ocean waters), but varies randomly for a given [C] value.

3.2.2 backscattering of detritus, mineral and others, $bb_{dm}(\lambda)$

$$bb_{dm}(\lambda) = \tilde{b}_{dm}\, b_{dm}(\lambda)$$
$$b_{dm}(\lambda) = b_{dm}(550)\left(\frac{550}{\lambda}\right)^{n2}. \tag{13}$$

Value of $\tilde{b}_{dm}$ depends on the selected phase function, and is 0.0183 when Petzold average particle phase function [*Mobley*, 1994; *Morel and Gentili*, 1991] is used. As above, $b_{dm}(550)$ and n_2 are created as follow,

$$b_{dm}(550) = p_4[C]^{0.766}, \tag{14}$$

with p_4 randomly valued between 0.06 and 0.6 for any [*C*] value. So values of $b_{dm}(550)$ are not fixed for a given [*C*].

n_2 is generated with

$$n_2 = -0.5 + \frac{2.0 + 1.2\Re_4}{1 + [C]^{0.5}}, \tag{15}$$

and $\Re_4$ is another random number between 0 and 1. n_2 is in a range of -0.2 to 2.2, but varies randomly for each [*C*]. Since $\Re_3$ and $\Re_4$ are independent random values, n_1 does not necessarily equal to n_2 for a given [*C*] value. Figure 5 presents the values and distribution of particulate backscattering coefficient at 550 nm ($bb_{ch}(550) + bb_{dm}(550)$) of the data set. Note the wide variation for each [*C*] value, generally consistent with the observations of Gordon and Morel [*Gordon and Morel*, 1983] and Loisel and Morel [*Loisel and Morel*, 1998].

With the above models and parameterizations, absorption and scattering coefficients for the given [*C*] values are created.

4. HydroLight simulation of AOP

The HydroLight [*Mobley*, 1995] numerical simulation code is used for the generation of AOPs, which include the remote-sensing reflectance (R_{rs}, ratio of water-leaving radiance to downwelling irradiance just above the surface), sub-surface remote-sensing reflectance (r_{rs}, ratio of upwelling radiance to downwelling irradiance just below the surface), and irradiance reflectance (R, ratio of upwelling irradiance to downwelling irradiance just below the surface). In the HydroLight runs, solar input is simulated with

the Gregg and Carder [*Gregg and Carder*, 1990] model, and the sky is assumed cloud free. A wind speed of 5 m/s is applied, and the water body is assumed homogeneous. Spectral bands are set from 400 nm to 700 nm, with a spacing of 10 nm. Initially, inelastic scatterings (such as Raman scattering, chlorophyll fluorescence, etc.) are excluded. These contributions, however, could be added in the future runs. Table 1 summarizes the above settings that used for the HydroLight runs.

Note that, the HydroLight generated reflectance spectra are not simply a function of [*C*], but a function of the IOPs, and the IOPs are determined by the combined effects of the values of [*C*], $p_{1\text{-}4}$, and $n_{1\text{-}2}$. This indicates, for two waters with the same [*C*] value, the synthesized reflectance may or may not be the same, as generally observed in the field.

However, the above simulated data certainly does not cover all possible natural waters, and not necessarily match all natural situations. Nevertheless, as the models and parameters are based on extensive field measurements, the IOP-AOP data should be consistent with a wide range of field observations. More importantly, this IOP-AOP data set has no errors from measurement mismatch or processing, which are common among *in situ* data.

5. Data files

Two IOP_AOP data files in Microsoft Excel format are created, with IOP_AOP_Sun30.xls for the Sun at 30^o from zenith, and IOP_AOP_Sun60.xls for the Sun at 60^o from zenith. Each page is pretty much self-descriptive. For questions regarding quantity definitions, please refer to Kirk [*Kirk*, 1994], Mobley [*Mobley*, 1994], and Bukata et al. [*Bukata et al.*, 1995].

References:

Babin, M., D. Stramski, G.M. Ferrari, H. Claustre, A. Bricaud, G. Obolensky, and N. Hoepffner, Variations in the light absorption coefficients of phytoplankton, nonalgal particles, and dissolved organic matter in coastal waters around Europe, *J. Geophy. Res.*, *108*, 4:1-20, 2003.

Bricaud, A., M. Babin, A. Morel, and H. Claustre, Variability in the chlorophyll-specific absorption coefficients of naturnal phytoplankton: Analysis and parameterization, *J. Geophy. Res.*, *100*, 13321-13332, 1995.

Bricaud, A., A. Morel, M. Babin, K. Allali, and H. Claustre, Variations of light absorption by suspended particles with chlorophyll a concentration in oceanic (case 1) waters: Analysis and implications for bio-optical models, *J. Geophy. Res.*, *103*, 31033-31044, 1998.

Bricaud, A., A. Morel, and L. Prieur, Absorption by dissolved organic matter of the sea (yellow substance) in the UV and visible domains, *Limnol. Oceanogr.*, *26*, 43-53, 1981.

Bukata, R.P., J.H. Jerome, K.Y. Kondratyev, and D.V. Pozdnyakov, *Optical Properties and Remote Sensing of Inland and Coastal Waters*, CRC Press, Boca Raton, FL, 1995.

Carder, K.L., F.R. Chen, Z.P. Lee, S.K. Hawes, and D. Kamykowski, Semianalytic Moderate-Resolution Imaging Spectrometer algorithms for chlorophyll-a and absorption with bio-optical domains based on nitrate-depletion temperatures, *J. Geophy. Res*, *104*, 5403-5421, 1999.

Carder, K.L., S.K. Hawes, K.A. Baker, R.C. Smith, R.G. Steward, and B.G. Mitchell, Reflectance model for quantifying chlorophyll a in the presence of productivity degradation products, *J. Geophys. Res*, *96*, 20599-20611, 1991.

Doerffer, R., K. Heymann, and H. Schiller, Case 2 water algorithm for the medium resolution imaging spectrometer (MERIS) on ENVISAT, ESA report ENVISAT validation workshop, 2002.

Fischer, J., and F. Fell, Simulation of MERIS measurements above selected ocean waters, *Int. J. Remote Sensing*, *20* (9), 1787-1807, 1999.

Gordon, H.R., and A. Morel, *Remote assessment of ocean color for interpretation of satellite visible imagery: A review*, 44 pp., Springer-Verlag, New York, 1983.

Gregg, W.W., and K.L. Carder, A simple spectral solar irradiance model for cloudless maritime atmospheres, *Limnol. Oceanogr.*, *35*, 1657-1675, 1990.

Kirk, J.T.O., *Light & Photosynthesis in Aquatic Ecosystems*, University Press, Cambridge, 1994.

Loisel, H., and A. Morel, Light scattering and chlorophyll concentration in Case 1 waters: A reexamination, *Limnol. Oceanogr.*, *43*, 847-858, 1998.

Mobley, C.D., *Light and Water: radiative transfer in natural waters*, Academic Press, New York, 1994.

Mobley, C.D., Hydrolight 3.0 Users' Guide, SRI International, Menlo Park, Calif., 1995.

Morel, A., Optical properties of pure water and pure sea water, in *Optical aspects of oceanography*, edited by N.G. Jerlov, and Nielsen, E. S., pp. 1-24, Academic, New York, 1974.

Morel, A., and B. Gentili, Diffuse reflectance of oceanic waters: its dependence on sun angle as influenced by the molecular scattering contribution, *Applied Optics*, *30*, 4427-4438, 1991.

Oishi, T., Y. Takahashi, A. Tanaka, M. Kishino, and A. Tsuchiya, Relation between the backward- as well as total scattering coefficients and the volume scattering functions by cultured phytoplankton, *J. School Mar. Sci. Technol. Tokai Univ.*, *53*, 1-15, 2002.

Pope, R., and E. Fry, Absorption spectrum (380 - 700 nm) of pure waters: II. Integrating cavity measurements, *Applied Optics*, *36*, 8710-8723, 1997.

Prieur, L., and S. Sathyendranath, An optical classification of coastal and oceanic waters based on the specific spectral absorption curves of phytoplankton pigments, dissolved organic matter, and other particulate materials, *Limnol. Oceanogr.*, *26*, 671-689, 1981.

Roesler, C.S., and E. Boss, Spectral beam attenuation coefficient retrieved from ocean color inversion, *Geophys. Res. Lett.*, *30* (9), 1468, 2003.

Roesler, C.S., M.J. Perry, and K.L. Carder, Modeling in situ phytoplankton absorption from total absorption spectra in productive inland marine waters, *Limnol. Oceanogr.*, *34*, 1510-1523, 1989.

Sathyendranath, S., L. Prieur, and A. Morel, A three-component model of ocean colour and its application to remote sensing of phytoplankton pigments in coastal waters, *Int. J. Remote Sensing*, *10*, 1373-1394, 1989.

Stramski, D., A. Bricaud, and A. Morel, Modeling the inherent optical properties of the ocean based on the detailed composition of the planktonic community, *Applied Optics*, *40*, 2929-2945, 2001.

Voss, K.J., A spectral model of the beam attenuation coefficient in the ocean and coastal areas, *Limnol. Oceanogr.*, *37* (3), 501-509, 1992.

Table 1. Parameters for IOP creation and HydroLight simulation.

Parameter	**Values or Ranges**
Sun angle (from zenith)	30^o; 60^o
Sensor viewing direction	nadir
Wind (m/s)	5
Wavelength (nm)	400 – 700, every 10 nm
[*C*] (μg/l) --- phytoplankton concentration	0.03; 0.05; 0.07; 0.1; 0.15; 0.2; 0.3; 0.5; 0.7; 1.0; 1.5; 2.0; 3.0; 5.0; 7.0; 10.0; 15.0; 20.0; 25.0; 30.0. (500 points)
$a_{ph}(\lambda)$ --- phytoplankton absorption spectrum	based on measurements
$a_{dm}(440)$ --- detritus/mineral absorption at 440 nm	modeled
S_{dm} --- spectral slop of detritus/mineral absorption	0.007 – 0.015 nm^{-1}
$a_g(440)$ --- gelbstoff absorption at 440 nm	modeled
S_g --- spectral slop of gelbstoff absorption	0.010 – 0.020 nm^{-1}
$c_{ph}(555)$ --- phytoplankton beam-attenuation coefficient at 555 nm	modeled
n_1 --- exponential exponent of $c_{ph}(\lambda)$	-0.1 – 2.0
phytoplankton scattering phase function	1% *bb*/*b* Fournier-Forand
$bb_{dm}(555)$ --- detritus/mineral backscattering at 555	modeled
n_2 --- exponential exponent of $bb_{dm}(\lambda)$	-0.2 – 2.2
detritus/mineral phase function	Petzold particle average
Inelastic scattering	without

Figures

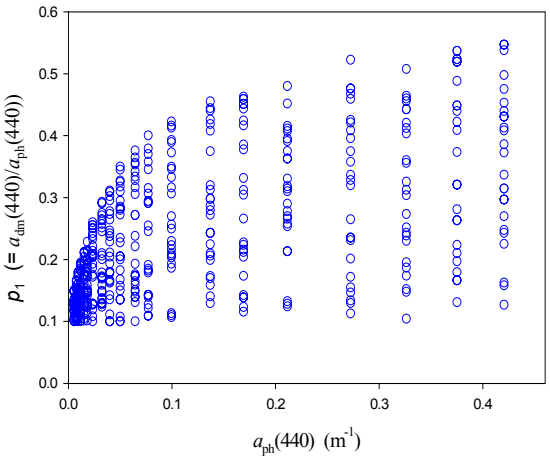

Figure 1. Values and distribution of p_1.

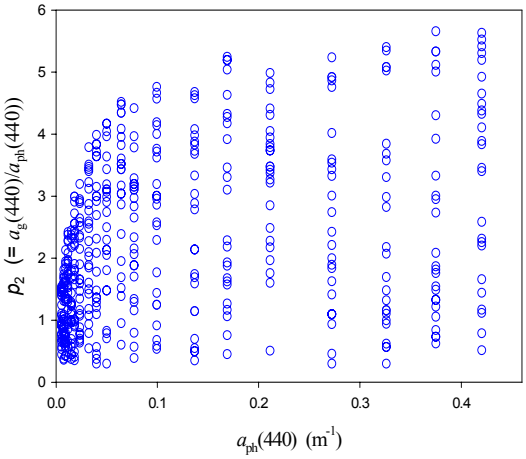

Figure 2. Values and distribution of p_2.

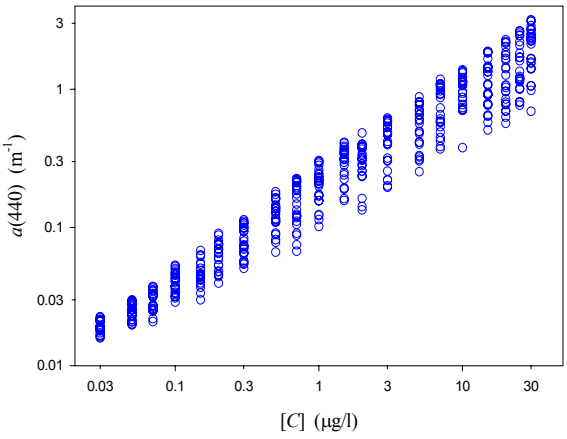

Figure 3. Values and distribution of $a(440)$.

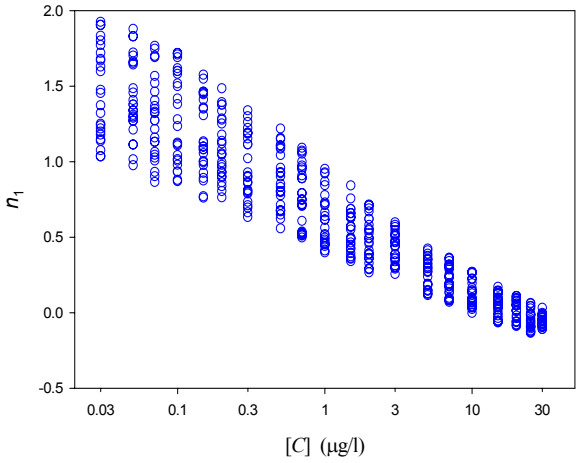

Figure 4. Values and distribution of n_1.

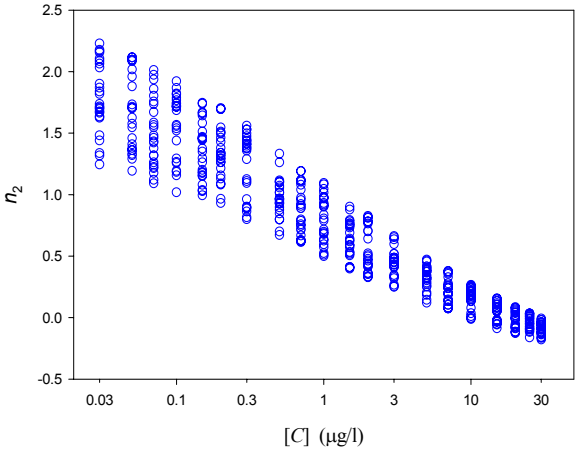

Figure 5. Values and distribution of n_2.

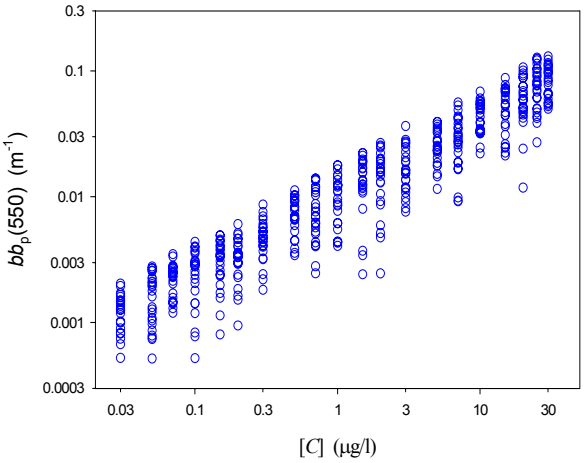

Figure 6. Values and distribution of $bb_p(550)$.